	SAKARYA UNIVERSITY **DISASTER MANAGEMENT APPLICATION AND RESEARCH CENTER**

PRELIMINARY SEISMOLOGICAL REPORT ON THE NOVEMBER 12, 2017 NORTHERN IRAQ/WESTERN IRAN EARTHQUAKE

REPORT NUMBER: 2017-3

Murat UTKUCU

SAKARYA

November 2017

SUMMARY

The November 12, 2017 Northern Iraq/Western Iran earthquake occurred along the northwestern part the Zagros Thrust Zone near the political boundary between Iraq and Iran and caused hundreds of deaths and thousands of injuries and building damages and collapses, especially in Kermanshah province of Iran. Although there have been no $M \geq 7.0$ earthquake since 1900, destructive earthquakes with comparable magnitude such as 1058 Mosul, 1263 Mardin, 1572 Halepçe, 1666 Ninova earthquakes, shook the source region in the historical period. Finite-fault inversion of the teleseismic broadband waveforms of the earthquake has indicated that the rupture covers a fault area of 50 km by 15 km and confined to depths below 20 km with slip as high as 9 m at hypocentral area. The rupture was mainly toward south (or toward Iran) providing plausible explanation for damage distribution. The earthquake released a seismic moment of 1.05×10^{20} Nt m ($M_W \approx 7.3$). It is suggested that the earthquake was due to displacement along the detachment surface between the sedimentary cover and underlying basement. The slip model further indicates that though the northern part of the faulting dominantly thrusting the southern half is dominantly dextral.

1. INTRODUCTION

Convergence between the Arabian Plate and the Eastern Anatolia and Iranian Plateau takes place along the Bitlis Thrust Zone and Zagros Thrust Zone (ZTZ), respectively (Fig. 1) (Vernant et al. 2004; Reilinger et al. 2006; Nissen et al. 2011; Mouthereau et al. 2012). The ZTZ is the 1,500-km-long fold and thrust belt, which lies in the western Iran and extends into the northern Iraq. Nevertheless, not all of the convergence, which is approximately 22 mm/year, is accommodated through crustal shortening and thickening by the ZTZ and a part of the convergence is transferred to the Alborz and Kopet Dagh Thrust Zones in the Northern Iran by N-S striking strike-slip faults in the Iranian Plateau. GPS studies have indicated that crustal shortening along the ZTZ is not evenly distributed. The shortening is 9 mm/year along the southeastern section of the ZTZ and gets smaller in the middle and the northeastern parts to values of 7 and 4 mm/year, respectively (Vernant et al. 2004; Reilinger et al. 2006).

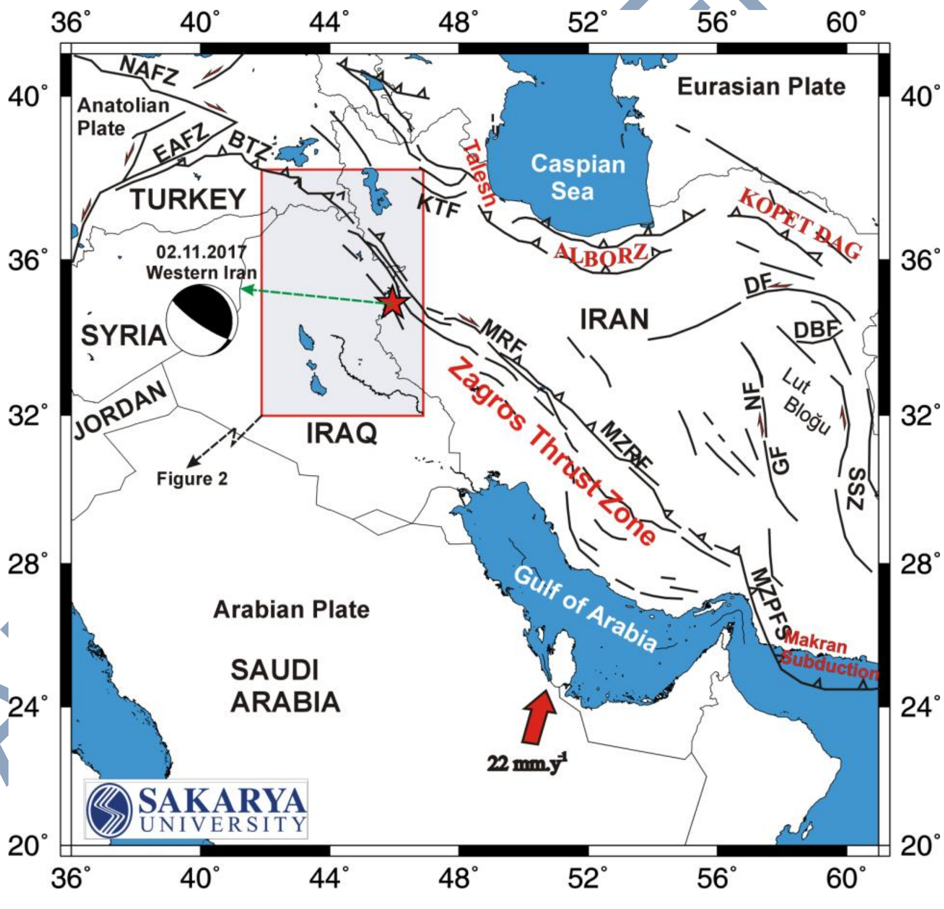

Figure 1. Major tectonic elements of the Middle East region. *MRF* Main Recent Fault, *MZRF* Main Zagros Reverse Fault, *MZPFS* Minab-Zendan-Palami Fault System, *DBF* Dasht-e Bayaz Fault, *DF* Doruneh Fault, *BTZ* Bitlis Thrust Zone, *NAFZ* North Anatolian Fault Zone, *EAFZ* East Anatolian Fault Zone, *NF* Nayband Fault, *GF* Gowk Fault, *SSZ* Sistan Suture Zone, *KTF* Northern Tabriz Fault.

The Main Recent Fault, strike-slip fault zone lying parallel to the ZTZ, is another conspicuous tectonic property of the region accommodating boundary parallel component of the convergence, which is oblique (Fig.1). Reilinger et al. (2006) calculated 3 mm/year right-lateral motion along the fault in the northwestern part of the ZTZ.

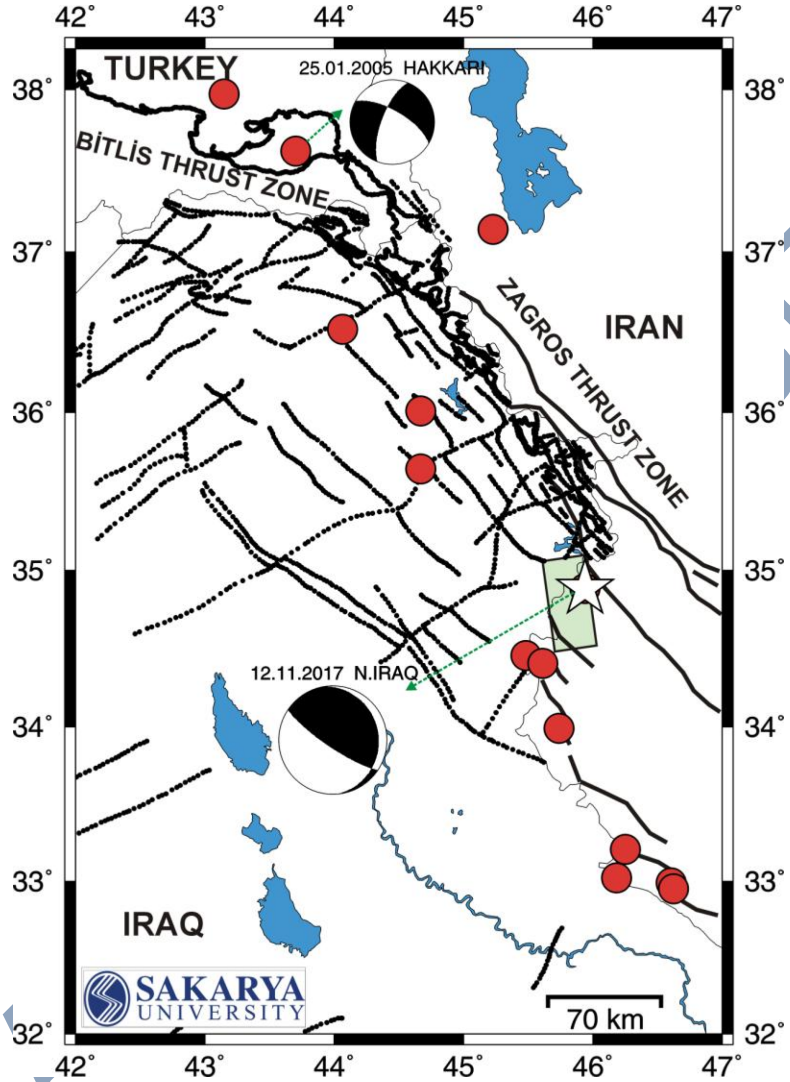

Figure 2. Seismotectonic map of the 2017 Northern Iraq/Western Iran earthquake (star) source region. Red circles show the epicenters of the $M \geq 5.0$ earthquakes available in the USGS-NEIC catalogue. Green shaded rectangle indicate model fault extend used in the teleseismic finite-fault inversion. Red outlined rectangle demonstrates the map area shown in Fig. 4.

The 12 November 2017 Northern Iraq/Western Iran earthquake (M_W=7.3) is the only $M \geq 7.0$ earthquake that occurred along the northwestern part the ZTZ in the instrumental period (Fig. 2). The largest earthquake that occurred in the near source region is the January 11, 1967 earthquake (M=6.1), which was located about 100 km south of the 2017 earthquake's epicenter. Nevertheless, destructive earthquakes such as 1058 Mosul, 1263 Mardin, 1572 Halepçe, 1666 Ninova earthquakes, occurred in the historical period (Ambraseys 2009). These earthquakes have more or less same magnitude as the 2017 earthquake.

Preliminary source mechanism solutions for the earthquake indicate oblique thrusting with right-lateral component over a fault plane dipping shallowly to the northeast (Fig. 2; Table 1). USGS-NEIC CMT solution revealed a centroid depth of 21.5 km. The earthquake caused hundreds of deaths (the latest reports indicate over 500) and thousands of injuries and building damages and collapses, especially in Kermanshah province of Iran. No surface ruptures have been reported so far. It has been common for the earthquakes along the ZTZ to occur without coseismic surface faulting (Nissen et al. 2010). Therefore we depend on the seismological studies for geometry and extend of the earthquake ruptures.

Table 1. Source parameters of the November 12, 2017 Northern Iraq/Western Iran earthquake.

	USGS-NEIC	GCMT	This study
Latitude (^{o})	34.886		
Longitude (^{o})	45.941		
Depth (km)	23.2		
Strike (^{o})	352	351	
Dip (^{o})	16	10	
Rake (^{o})	138	143	
CMT depth	21.5	17	
M_o (x10^{20} Nm)	1.23	1.72	1.05
*M*w	7.3	7.4	7.3

2. TELESEISMIC FINITE-FAULT INVERSION

A finite-fault inversion methodology developed by Kikuchi et al. (2003) is used to find finite-fault rupture model of the 2017 earthquake. The finite source of the target earthquake is represented by grid plane with equally spaced 12 x 6 grid points along the strike and the dip, respectively. The strike, dip and rake angle of the grid plane are assigned as 358^o, 16^o and 138^o, respectively, based on USGS-NEIC CMT solution (Table 1). Nevertheless, rake angle can vary ±45^o of the defined value in the modelling so that a rupture model with variable rake angle for each grid point could be obtained. The grid plane covers the depth range 17.5km-24.4 km. The modelling was carried out by incorporating 5 consecutive time windows; slip rise-time of each is represented by an isosceles triangle of 1 sec rise and fall. A maximum rupture velocity of 3.5 km/s is defined for the modelling. Green's functions have been calculated using the reflectivity method (Koketsu, 1985) assuming the crustal velocity structure given by Abdulnabi et al. (2013) (Table 2). The epicentre determined by USGS-NEIC is selected as the rupture initiation point.

Table 2. Crustal velocity structure utilized in the inversion of the 17 November 2017 Western Iran earthquake (Abdulnabi et al., 2013).

Thickness(km)	V_P (km/s)	V_s (km/s)	ρ (gr/cm^3)
1.9	3.92	2.19	2.31
4.1	5.75	3.20	2.65
10.0	6.63	3.70	2.88
23	6.90	3.85	2.95
-	7.71	4.10	3.21

We use the teleseismic broadband *P* and *SH* displacement waveforms retrieved from the IRIS Data Management Centre for the earthquake. The data is corrected for the instrument responses and bandpass filtered with corner frequencies at 0.01 to 0.5 Hz. A sampling interval of 0.50 is used. 30 *P* and 2 *SH* waveforms are included in the inversion. Considering the size of the earthquake and the finite-fault model parameterization, a record length of 50 s is chosen for the inversion.

Several inversion trials have been carried out to find grid point corresponding to the rupture initiation point. It has been obtained that the eighth grid point along the strike (rupture propagation mainly toward south) and fifth grid point along the dip as the rupture initiation is the best assumption regarding the data used. The total seismic moment and average rake angle are calculated as 1.05 x 10^{20} Nt m (M_W≈7.3) and 144^o, respectively (Fig. 3). The average rake angle suggests that the rupture was oblique with thrusting and dextral component in accordance with the seismotectonics of the source region controlled by the oblique convergence of the Arabian Plate along the ZTZ.

The coseismic slip distribution found in the study is shown in Fig. 3 along with comparison of the observed waveforms with synthetic waveforms calculated from the slip model. The slip model indicates that the rupture confined to depths below 20 km with maximum slip (about 9 m) occurred at the hypocenter. The major rupture is 50 km in length and 15 km in width and two third of its propagation is toward south (or toward Iran). This finding explains why Iran took brunt of the damage from the earthquake. Near horizontal dipping and depth of the faulting suggests that it reflects displacement along the detachment surface. Possibly, the active shortening takes place

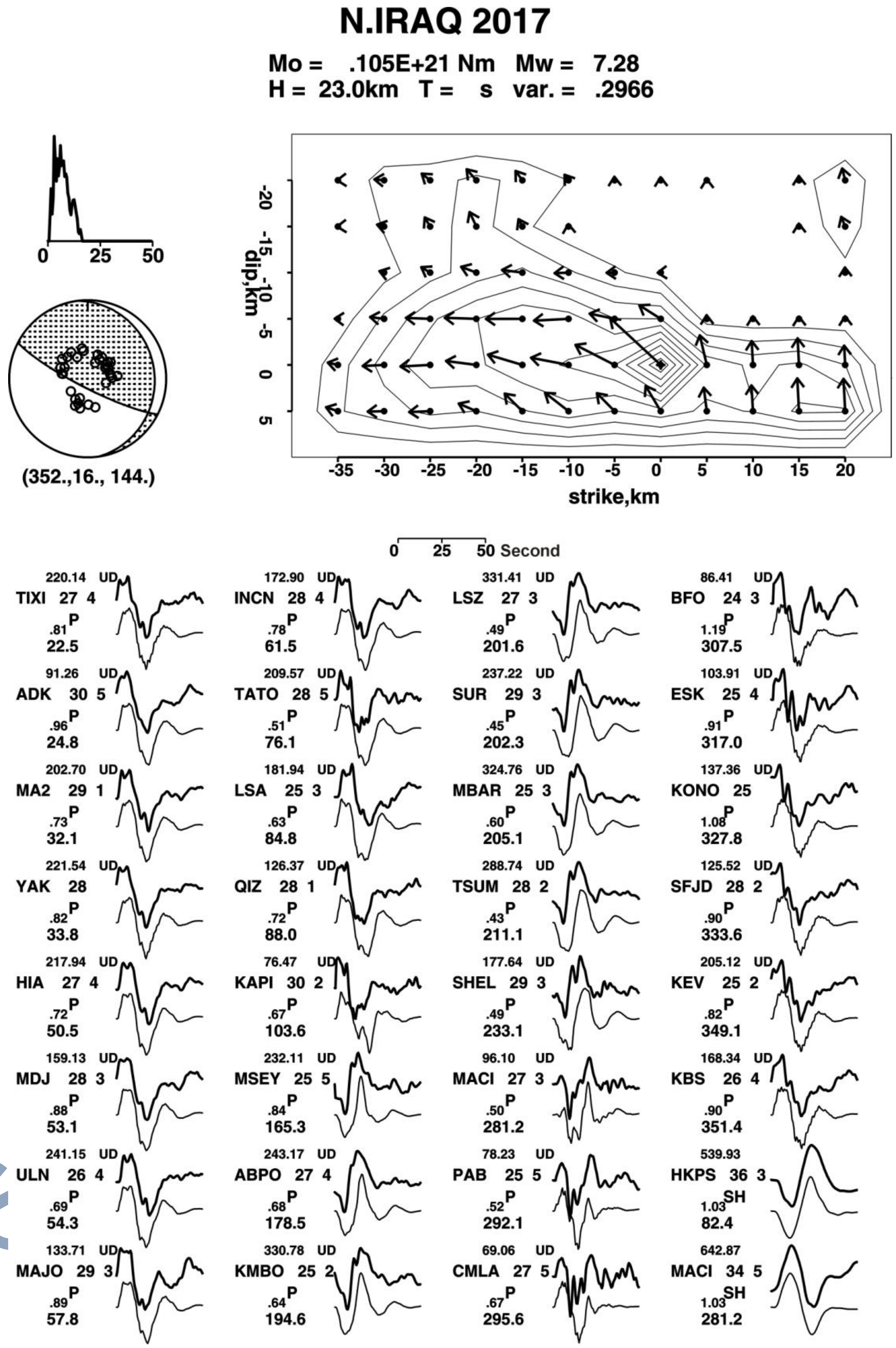

Figure 3. Moment-rate function and source mechanism (top left) and slip distribution model (top right) of the November 12, 2017 Norther Iraq/Western Iran earthquake obtained in the study. Comparison of the observed waveforms (black) with synthetic waveforms (gray) calculated from the slip distribution model is shown in the bottom. Slip is contoured at 1 m interval and only slips equal and larger than 1 m are shown.

within the sedimentary cover above detachment of the basement as in the middle and southern part of the ZTB (Nissen et al. 2011 and 2014). This could be better understood from Fig. 4 in which 3-D view of the earthquake source region. The slip model further indicates that though the northern part of the faulting dominantly thrusting the southern half is dominantly dextral.

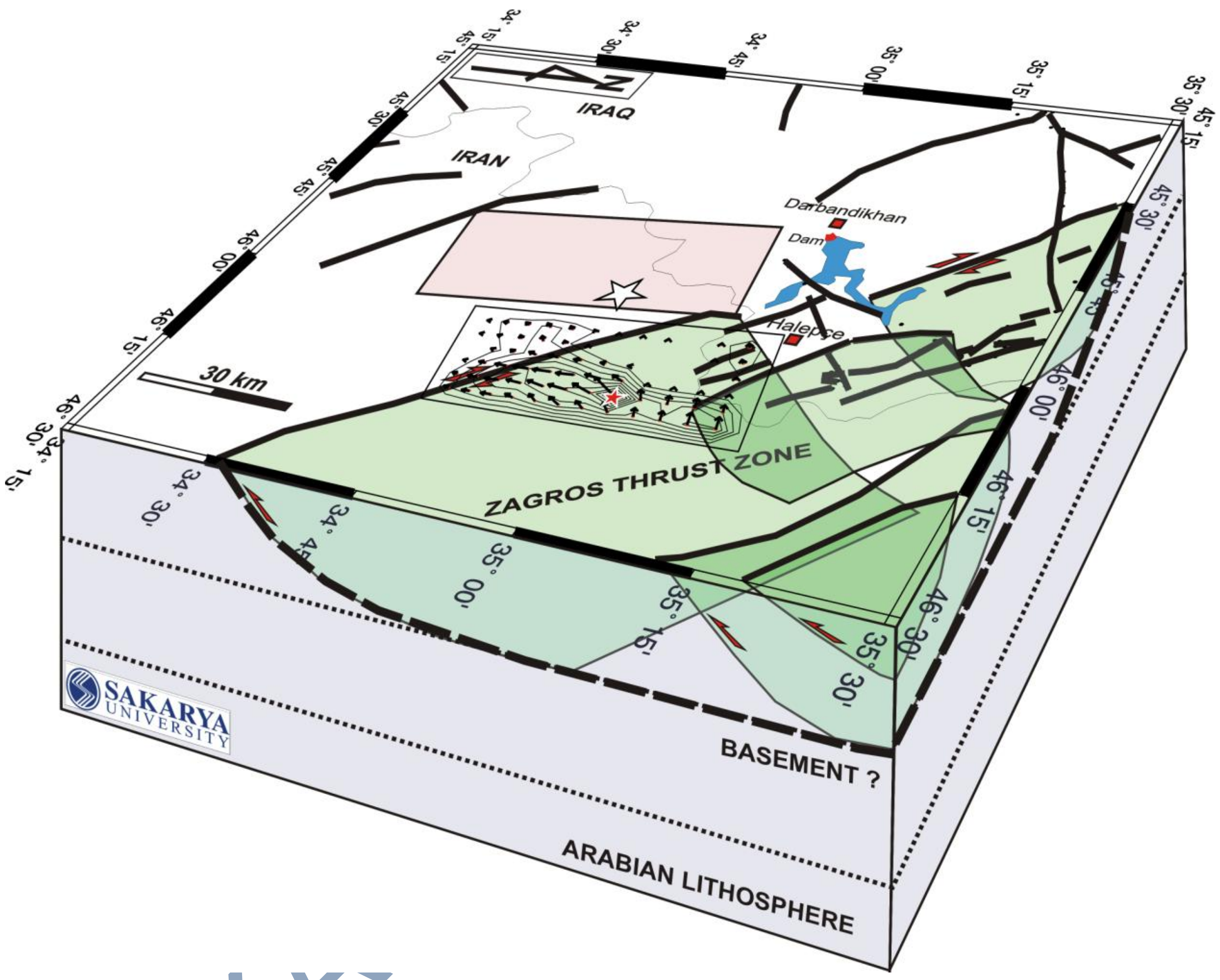

Figure 4. 3-D representative view of the November 12, 2017 Northern Iraq/Western Iran earthquake's source region with the slip model embedded.

CONCLUSIONS

The 12 November 2017 Western Iran earthquake (M_W=7.3) that occurred along the northwestern part the ZTZ with heavy human casualties and building damage. Finite-fault inversion of the teleseismic broadband body waveforms of the earthquake has indicated that the rupture confined to depths below 20 km with slip as high as 9 m at hypocentral depths.. The rupture was mainly toward south (or toward Iran) and released a seismic moment of 1.05 x 10^{20} Nt m (M_W≈7.3). Teleseismic inversion findings suggest that the earthquake reflects displacement along the detachment surface between the sedimentary cover and underlying basement. The slip model further indicates that though the northern part of the faulting dominantly thrusting the southern half is dominantly dextral.

Acknowledgement

This study was funded by Research Fund of the Sakarya University.

REFERENCES

Abdulnaby, W., Mahdi, H., Numan, N.M.S and Al-Shukri, H. (2013). Seismotectonics of the Bitlis-Zagros Thrust Belt in Northern Iraq and surrounding region from moment tensor analysis. *Pure and Applied Geophysics*, doi 10.1007/s00024-013-0688-4.

Ambraseys, N. N., (2009). Earthquakes in the eastern Mediterranean and the Middle East: a multidisciplinary study of 2,000 years of seismicity, Cambridge University Press

Kikuchi, M., M. Nakamura, and K. Yoshikawa (2003). Source rupture processes of the 1944 Tonankai earthquake and the 1945 Mikawa earthquake derived from low-gain seismograms, *Earth Planets Space*, 55, 159–172.

Koketsu, K. (1985). The extended reflectivity method for synthetic nearfield seismograms, *J. Phys. Earth*, 33, 121– 131.

Mouthereau, F., Lacombe, O., and Vergés, J. (2012). Building the Zagros collisional orogen: timing, strain distribution and the dynamics of Arabia/Eurasia plate convergence. *Tectonophysics*, 532, 27-60.

Nissen, E., Jackson, J., Jahani, S., and Tatar, M. (2014). Zagros "phantom earthquakes" reassessed—The interplay of seismicity and deep salt flow in the Simply Folded Belt? *Journal of Geophysical Research: Solid Earth*, 119(4), 3561-3583.

Nissen, E., Tatar, M., Jackson, J., Jahani, S., and Allen, M.A. (2011). New views on earthquake faulting in the Zagros Thrust fold-and-thrust belt of Iran. *Geophysical Journal International*, 186, 928-944.

Nissen, E., Yamini-Fard, F., Tatar, M., Gholamzadeh, A., Bergman, E., Elliott, J., Jackson, J., and Parsons, B. (2010). The vertical separation of mainshock rupture and microseismicity at Qeshm island in the Zagros fold-and-thrust belt, Iran. *Earth and Planetary Science Letters* 296, 181–194

Reilinger, R., McClusky, S., Vernant, P., Lawrence, S., Ergintav, S., Cakmak, R., Ozener, H., Kadirov, F., Guliev, I., Stepanyan, R., Nadariya, M., Hahubia, G., Mahmoud, S., Sakr, K., ArRajehi, A., Paradissis, D., Al-Aydrus, A., Prilepin, M., Guseva, T., Enren, E., Dmitrotsa, A., Filikov, S.V., Gomez, F., Al-Ghazzi, R., Karam, G., (2006.) GPS constraints on continental deformation in the Africa-Arabia-Eurasia continental collision zone and implications for the dynamics of plate interactions. *Journal of Geophysical Research*, 111, B05411, doi:10.1029/2005JB004051.

USGS-NEIC https://earthquake.usgs.gov/earthquakes/eventpage/us2000bmcg#moment-tensor

Vernant, P., Nilforoushan, F., Hatzfeld, D., Abbassi, M. R., Vigny, C., Masson, F., and Tavakoli, F. (2004). Present-day crustal deformation and plate kinematics in the Middle East constrained by GPS measurements in Iran and northern Oman. *Geophysical Journal International*, 157(1), 381-398.